Chain Conformation and Aggregation Structure Regulation of an Efficient Acceptor-Acceptor Typed Photovoltaic Polymer

Xiaoman Gui,[a] Jianling Ni,[a] Han Shen,[a] Bing Zheng,[a] Shisong Sun,[a] Panfeng Gao,[b] Lijun Huo*[a]

X. Gui, J. Ni, H. Shen, B. Zheng, S. Sun, Prof. L. Huo

School of Chemistry Beihang University Beijing 100191, PR China. E-mail: huolijun@buaa.edu.cn

Prof. P. Gao

School of Environmental Science and Engineering, Xiamen University of Technology, Xiamen, China

1. Materials and synthesis

All chemicals, unless otherwise specified, were purchased from commercial resources and used as received. Toluene was distilled from sodium benzophenone under nitrogen before using. The compound A_1, A_2 and A_3 were purchased from Woer Jiming research institute.

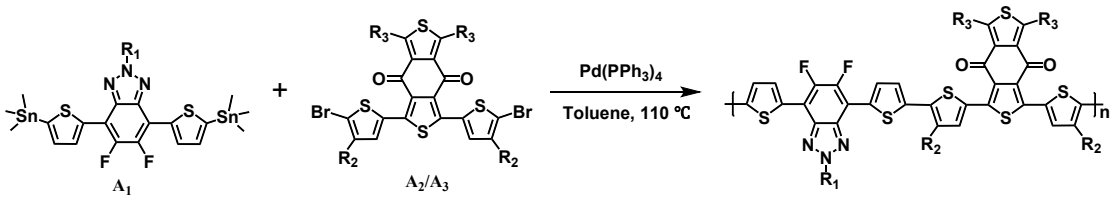

Scheme S1. The synthetic routes of the copolymers.

Synthesis of the copolymer P94

The A_1 (95.7 mg, 0.11 mmol), A_2 (109.0 mg, 0.11 mmol), $Pd(PPh_3)_4$ (5%mol) were

dissolved into toluene of 8 mL in a flask under nitrogen. The solution was flushed with nitrogen for an additional 15 min. Then, the reaction mixture was stirred for 24 h at 110 °C. Subsequently, the polymer was collected by filtration and purified by washing, extracted on a Soxhlet extractor with methanol and hexane in succession. The final product was obtained by precipitating the chloroform solution in methanol, collected by filtration and dried in vacuo to get the **P94** as dark red solid (yield: 51%). Calculated for $C_{80}H_{107}F_2N_3O_2S_6$: C, 69.98; H, 7.85; N, 3.06. Found: C, 69.44, H, 7.79, N, 3.01. M_n = 16.4K; polydispersity = 2.29.

Synthesis of the copolymer P95

The A_1 (113.1 mg, 0.13 mmol), A_3 (128.8 mg, 0.13 mmol), $Pd(PPh_3)_4$ (5%mol) were dissolved into toluene of 10 mL in a flask under nitrogen. The solution was flushed with nitrogen for an additional 15 min. Then, the reaction mixture was stirred for 24 h at 110 °C. Subsequently, the polymer was collected by filtration and purified by washing, extracted on a Soxhlet extractor with methanol and hexane in succession. The final product was obtained by precipitating the chloroform solution in methanol, collected by filtration and dried in vacuo to get the **P95** as dark red solid (yield: 64%). Calculated for $C_{80}H_{107}F_2N_3O_2S_6$: C, 69.98; H, 7.85; N, 3.06. Found: C, 69.32, H, 7.81, N, 2.98. M_n = 17.5K; polydispersity = 1.99.

2. Characterization of materials

^{1}H NMR spectra were recorded on a Bruker AVANCE 300 MHz spectrometer using $CDCl_3$ as the solvent. The molecular weight of polymers was determined by gel permeation chromatography (GPC) relative to polystyrene standards with chloroform as the eluent. Thermal gravimetric analysis (TGA) was performed on a Perkin-Elmer Pyris 1 thermogravimetric analyzer. UV–vis absorption measurements were carried out on a Hitachi (model U-3010) UV–vis spectrophotometer. Cyclic voltammetric (CV) measurements were carried out in a conventional three-electrode cell using a platinum plate as the working electrode, a platinum wire as the counter electrode, and an Ag/Ag^+ electrode as the reference electrode on a Zahner IM6e Electrochemical workstation in a tetrabutylammonium hexafluorophosphate (Bu_4NPF_6) (0.1 M) acetonitrile solution at

a scan rate of 20 mV s^{-1}. The E^{ox} and E^{re} values were calibrated as Fc/Fc^{+} value was as internal standard. According to the following formula, we could calculate the HOMO/LUMO values:

HOMO=eE^{ox}+4.8 (v Ag/Ag^{+})-$E^{ox}{}_{Fc/Fc^{+}}$

LUMO=eE^{re}+4.8 (v Ag/Ag^{+})-$E^{re}{}_{Fc/Fc^{+}}$

3. Device Fabrication and Characterization

(1) Device Fabrication

An inverted architecture was fabricated with ITO/PEDOT:PSS/active layer/ PDINO/Ag. The ITO-coated glass substrates were sequentially ultrasonicated in soap water, deionized water, acetone, and isopropyl alcohol for at least 15 min, and ultimately dried in an oven overnight. The ITO-coated glass substrates were treated by uv-ozone for 10 min. Filter the PEDOT:PSS aqueous solution (Baytron P 4083, from HCStarck) through a 0.45 mm filter, and pre-coat it on the pre-cleaned ITO glass at 5000 rpm for 30 seconds, and then heat the ITO substrate in the air at 150°C annealing for 0.5 h. The polymer donor: ITIC-4Cl (D:A=1:1.1, 15 mg mL^{-1} in total) or the polymer donors: Y6 (D:A=1:1.2, 18 mg mL^{-1} in total) was dissolved in chloroform, adding 1-chloronaphthalene (CN) (0.7%, v/v) as additive). The blended solution was spin-coated on the PEDOT:PSS layer at 3000 rpm for 30s. It is then annealed at 110°C for 10 minutes. Then PNDIT-F3N methanol solution with a concentration of 0.3 mg mL-1 was deposited on the active layer at a speed of 3000 rpm for 30 seconds to provide a PDINO cathode modification layer. After cooling to room temperature, the sample was transferred to the evaporation chamber. Under the pressure of 1×10^{-5} Pa, about 100 nm of Ag electrode was evaporated and deposited. The device area is 4.0 mm^2. The active area of the devices is 4.0 mm^2. Current density-voltage (*J-V*) characteristics were measured by a Keithley 2400 Source Measure Unit, in N_2 atmosphere under an AM 1.5G solar simulator with an irradiation light intensity of 100mw·cm^{-2}. The external quantum efficiency (EQE) of the devices was measured by using a QEX10 solar cell EQE measurement system (PV measurements.Inc.). The light intensity at each wavelength was calibrated with a standard single-crystal Si photovoltaic cell.

(2) Space-Charge-Limited Current (SCLC)

The current density–voltage (J–V) characteristics of the hole or electron only devices are fitted by the Mott–Gurney law:

$$J = (9/8)\varepsilon_r\varepsilon_0\mu(V^2/L^3)$$

where J is the current density, ε_r is the dielectric permittivity of the active layer, ε_0 is the vacuum permittivity, L is the thickness of the active layer, μ is the mobility. $V=V_{app} - V_{bi}$, where V_{app} is the applied voltage, V_{bi} is the offset voltage (V_{bi} is 0 V here). The mobility can be calculated from the slope of the $J^{0.5}\sim V$ curves.

(3) Grazing Incidence Wide-Angle X-ray Scattering (GIWAXS) Characterization

GIWAXS measurements were performed at beamline 7.3.3 at the Advanced Light Source. Samples were prepared on Si substrates using identical blend solutions as those used in devices. The 10 keV X-ray beam was incident at a grazing angle of 0.12°-0.16°, selected to maximize the scattering intensity from the samples. The scattered x-rays were detected using a Dectris Pilatus 2M photon counting detector.

(4) Atomic force microscopy (AFM) Characterization

AFM images were investigated on a Dimension Icon AFM (Bruker) in a tapping mode.

(5) Transmission Electron Microscopy (TEM) Characterization

TEM images were performed on a JEOL JEM-1400 transmission electron microscope. TEM samples were prepared as follows: First, the active layer was spin cast on the top of ITO/PEDOT:PSS substrates; Then, the active layer film was peeled off and floated onto the surface of deionized water; Finally, the floated films were picked up on a carbon film 200 mesh copper grid for TEM measurements.

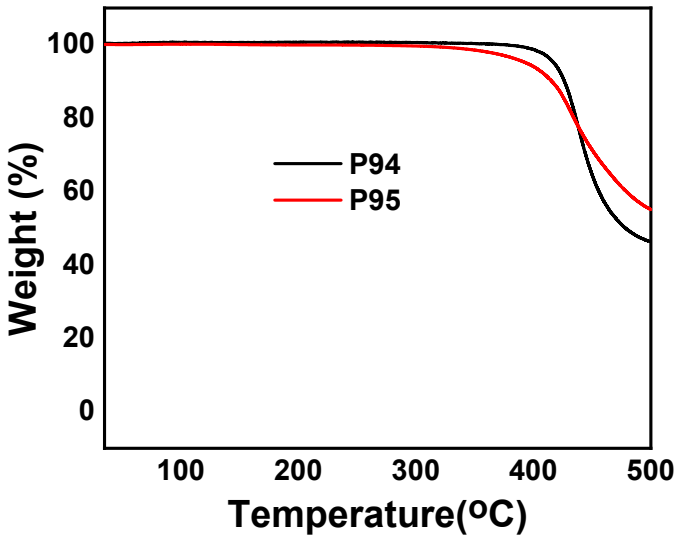

Figure S1. TGA plots of polymers with a heating rate of 20 °C/min under the inert atmosphere.

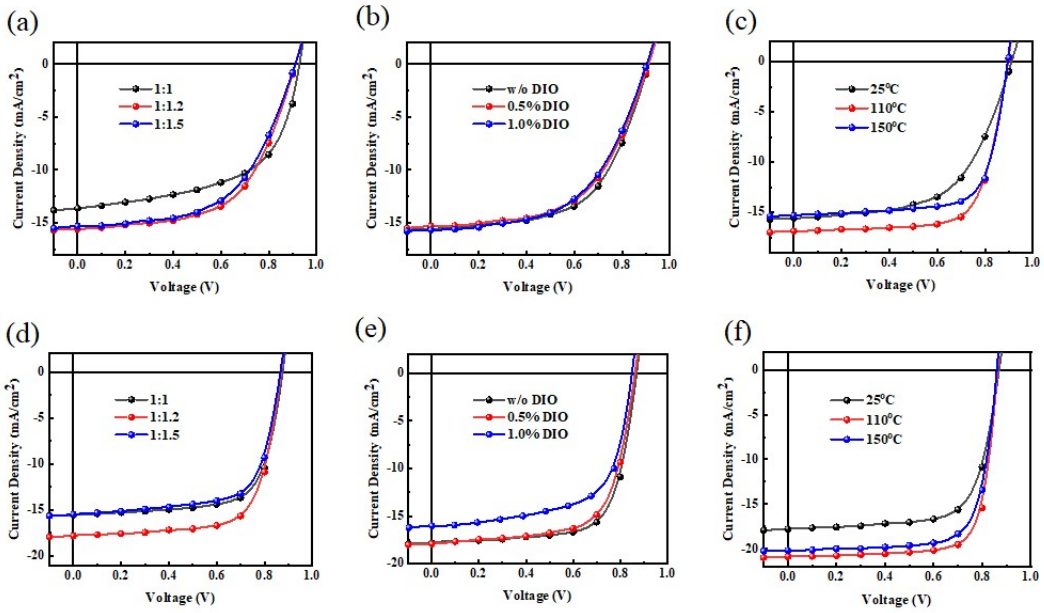

Figure S2. Photovoltaic performance of the OSCs based on P94:ITIC-4Cl and P95:ITIC-4Cl with different device fabrication conditions: (a), (d) donor:acceptor weight ratios; (b), (e) DIO additive; (c), (f) thermal annealing temperature.

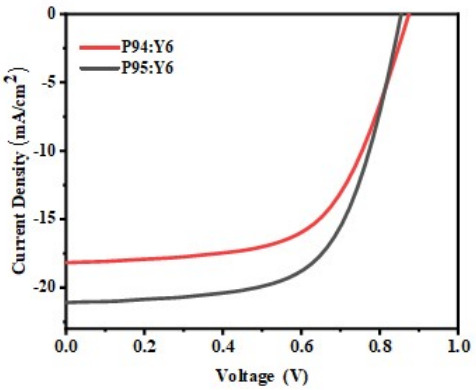

Figure S3. Photovoltaic performance of the OSCs based on P94:Y6 and P95:Y6 with optimized device conditions.

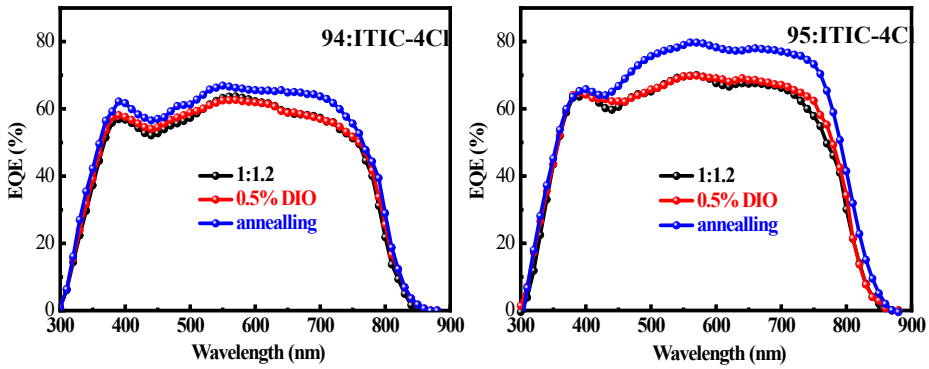

Figure S4. The external quantum efficiency (EQE) spectra of the devices based on (a) P94:ITIC-4Cl and (b) P95:ITIC-4Cl under various conditions.

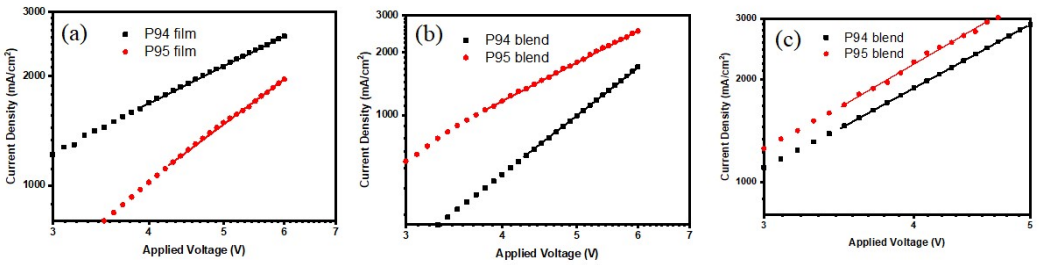

Figure S5. *J-V* characteristics of a) hole-only devices based on P94 and P95 neat films, b) hole-only devices based on the P94:ITIC-4Cl and P95:ITIC-4Cl blend films,

c) electron-only devices based on the P94:ITIC-4Cl and P95:ITIC-4Cl blend films.

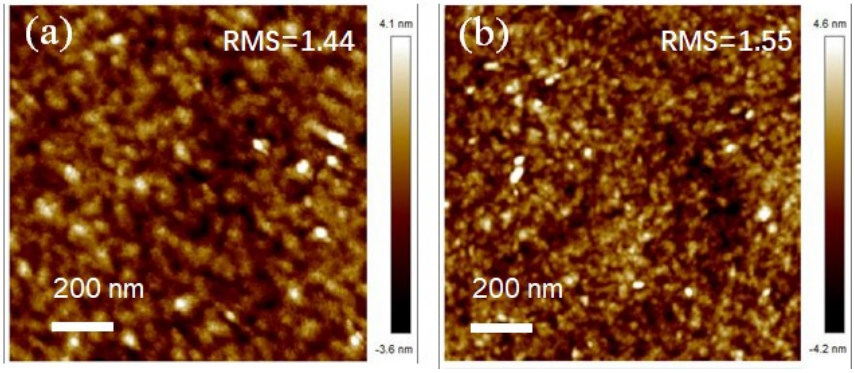

Figure S6. AFM height images of a) P94, b) P95 neat films.

Table S1 Photovoltaic performance of the devices based on 94: ITIC-4Cl with different weight ratios under the illumination of AM1.5G, 100 mW/cm^2.

94: ITIC-4Cl	V_{oc} (V)	J_{sc} (mA/cm^2)	FF (%)	PCE (%)
1:1	0.93	13.63	56.9	7.22 (7.04)
1:1.2	0.91	15.60	58.1	8.27 (8.09)
1:1.5	0.91	15.32	56.0	7.82 (7.80)

Table S2 Photovoltaic performance of the devices based on 94: ITIC-4Cl with different DIO under the illumination of AM1.5G, 100 mW/cm^2.

DIO (%)	V_{oc} (V)	J_{sc} (mA/cm^2)	FF (%)	PCE (%)
0%	0.91	15.60	58.1	8.27 (8.09)
0.5%	0.91	15.32	56.0	7.82 (7.74)
1%	0.90	15.68	54.2	7.65 (7.54)

Table S3 Photovoltaic performance of the devices based on 94: ITIC-4Cl with different temperature of thermal annealing under the illumination of AM1.5G, 100 mW/cm^2.

Temperature (°C)	V_{oc} (V)	J_{sc} (mA/cm^2)	FF (%)	PCE (%)
25	0.91	15.60	58.1	8.25 (8.09)
100	0.90	16.88	71.4	10.82 (10.75)
120	0.90	15.31	72.6	9.97 (9.94)

Table S4 Photovoltaic performance of the devices based on 95: ITIC-4Cl with different

weight ratios under the illumination of AM1.5G, 100 mW/cm^2.

95: ITIC-4Cl	V_{oc} (V)	J_{sc} (mA/cm^2)	FF (%)	PCE (%)
1:1	0.88	15.54	69.2	9.46 (9.30)
1:1.2	0.87	17.80	70.6	10.94 (10.75)
1:1.5	0.87	15.46	68.9	9.26 (9.11)

Table S5 Photovoltaic performance of the devices based on 95: ITIC-4Cl with different DIO under the illumination of AM1.5G, 100 mW/cm^2.

DIO (%)	V_{oc} (V)	J_{sc} (mA/cm^2)	FF (%)	PCE (%)
0%	0.87	17.80	70.6	10.94 (10.75)
0.5%	0.86	17.92	69.3	10.68 (10.44)
1%	0.85	16.21	63.3	8.72 (8.65)

Table S6 Photovoltaic performance of the devices based on 95: ITIC-4Cl with different temperature of thermal annealing under the illumination of AM1.5G, 100 mW/cm^2.

Temperature (°C)	V_{oc} (V)	J_{sc} (mA/cm^2)	FF (%)	PCE (%)
0%	0.87	17.80	70.6	10.94 (10.75)
100	0.86	20.87	75.3	13.51 (13.37)
150	0.86	20.18	74.5	12.93 (12.55)

Table S7. PCE values based on reported A_1-A_2 typed binary OSCs since 2013 year and the photovoltaic performance for P94 and P95 based devices.[1-18]

NO.	**Donor:acceptor**	V_{oc} **(V)**	J_{sc} **(mA/cm^2)**	**FF (%)**	**PCE (%)**	**Reference**
This work	**P95:ITIC-4Cl**	**0.86**	**20.87**	**75.3**	**13.51**	**------**
	P94:ITIC-4Cl	**0.90**	**16.88**	**71.4**	**10.82**	**------**
1	PffBT-DPP:[70]PCBM	0.74	12.5	74	6.8	1
2	PffBT-DPP:MeIC	0.78	4.5	58	2	1
3	TBT-DPP:$PC_{71}BM$	0.31	-3.82	32.1	0.39	2
4	FTBT-DPP:$PC_{71}BM$	0.63	-3.31	54.9	1.15	2
5	HFTBT-DPP:$PC_{71}BM$	0	0	0	0	2
6	PBTZ-TTz:IT-4F	0.86	11.8	57.9	5.9	3
7	PV2TC-BDD:IT-4F	0.87	18.83	69.97	11.50	4
8	PV2TC-FTAZ:IT-4F	0.71	20.49	58.57	8.56	4
9	PBDB-TAZ20:ITIC	0.87	19.03	73.5	12.34	5
10	PBDB-TAZ40:ITIC	0.84	18.46	71.5	11.27	5
11	PBTZ-4TC:ITIC-Th1	0.88	15.72	62.62	8.72	6

NO.	Donor:acceptor	V_{oc} (V)	J_{sc} (mA/cm^2)	FF (%)	PCE (%)	Reference
12	PBTZ-C4T:ITIC-Th1	0.84	16.59	66.65	9.34	6
13	PhI-ffBT:IT-4F	0.91	19.41	76	13.31	7
14	ffPhI-ffBT:IT-4F	0.94	19.01	71	12.74	7
15	PBDD-BTZ-1:ITIC-Th	0.83	10.0	54.7	4.6	8
16	PBDD-BTZ-2:ITIC-Th	0.94	13.2	67.9	8.4	8
17	PBDD-BTZ-3:ITIC-Th	1.07	11.9	56.7	7.3	8
18	P1:$PC_{71}BM$	0.61	11.32	58	4.0	9
19	P2:$PC_{71}BM$	0.68	9.25	47	3.0	9
20	P(DTPz-ID):$PC_{71}BM$	0.86	1.2	30.4	0.3	10
21	P(dDTPz-ID):$PC_{71}BM$	0.96	1.2	38	0.4	10
22	P(DTPz-DTBT):$PC_{71}BM$	0.6	7.1	43.1	1.8	10
23	P(dDTPzDTBT):$PC_{71}BM$	1.0	11.4	43.2	5.0	10
24	PB24-3TDC:ITIC-Th	0.9	16.8	68	10.3	11
25	PB68-3TDC:ITIC-Th	0.99	12.2	65	7.8	11
26	PTB7-Th:PIIG-NDI(OD)	0.82	5.06	36.3	1.70	12
27	PTB7-Th:PIIG-PDI(EH)	0.73	5.88	50.2	2.21	12
28	PTB7-Th:PIIG-PDI(OD)	0.72	8.22	44.2	2.68	12
29	P3HT:P1-C12	0.52	0.68	40.9	0.14	13
30	P3HT:P1-C20	0.54	0.69	41.5	0.15	13
31	P3HT:P2-C12	0.35	0.48	35.2	0.06	13
32	P3HT:P2-C20	0.38	0.51	39.1	0.07	13
33	PFDTBT:P1-C12	0.88	1.30	25.7	0.29	13
34	PFDTBT:P1-C20	0.88	1.36	25.7	0.31	13
35	PFDTBT:P2-C12	0.75	0.39	27.0	0.08	13
36	PFDTBT:P2-C20	0.76	0.42	27.4	0.09	13
37	P1:L8-BO	0.766	18.12	73.72	10.37	14
38	P3:L8-BO	0.742	22.80	74.30	12.56	14
39	PBTz-TC:IT-4F	0.86	20.56	66.55	11.69	15
40	PBTz-TC/IT-4F	0.86	20.54	68.18	11.96	15
41	PBTz-TTC:IT-4F	0.84	18.38	60.94	9.37	15
42	PBTz-TTC/IT-4F	0.84	18.47	61.40	9.52	15
43	PBTz-TC:IT-4F(TMB)	0.84	20.61	71.76	12.42	15
44	PBTz-TC/IT-4F(TMB)	0.84	20.91	72.69	12.81	15
45	PTBTfBTzSi:$PC_{71}BM$	0.94	14.36	66.0	8.91	16
46	PffBT4T:ITIC-Th	0.858	13.47	57.1	6.6	17
47	PffBT4T-B:ITIC-Th	0.972	15.59	61.8	9.4	17
48	PTT-FBTz:$PC_{71}BM$	0.848	7.40	41.9	2.63	18
49	PTTz-FBTz:$PC_{71}BM$	0.880	11.25	69.9	7.03	18

Table S8 Optimized photovoltaic performance of polymer blends (A_1-A_2 based

polymer donor and Y acceptor series)

Polymer donor	Acceptor	V_{oc} (V)	J_{sc} (mA·cm^{-2})	*FF* (%)	PCE (%)	Refs
PDTz-BDD	BTP-eC9	0.78	22.05	59.97	10.36	Chem. J. Chinese Universities, 2023, 44, 20230157
P1	L8-BO	0.766	18.12	73.72	10.37	Polym. Chem., 2023, 14, 4227–4234
P3	L8-BO	0.742	22.80	74.30	12.56	Polym. Chem., 2023, 14, 4227–4234
P94	Y6	0.864	18.33	63.14	10.01	This work
P95	Y6	0.851	21.08	65.02	11.66	This work

Table S9. The hole and electron mobility data and the ratio μ_h/μ_e of neat and blend films.

Polymers:ITIC-4Cl	μ_h (cm^2 V^{-1} s^{-1})	μ_e (cm^2 V^{-1} s^{-1})	μ_h/μ_e
P94 neat film	6.25×10^{-4}		
P95 neat film	1.06×10^{-3}		
P94 blend film	4.88×10^{-4}	1.34×10^{-3}	0.36
P95 blend film	8.03×10^{-4}	1.36×10^{-3}	0.59

Reference

[1] Pan L. H., Liu T., Wang J. Y., *et al*. Efficient Organic Ternary Solar Cells Employing Narrow Band Gap Diketopyrrolopyrrole Polymers and Nonfullerene Acceptors[J]. Chemistry of Materials, 2020, 32(17): 7309-7317

[2] Du J. P., Feng S. S., Qin P. J., *et al*. Bis(thien-2-yl)-2,1,3-benzothiadiazole-diketopyrrolopyrrole- based acceptor - acceptor conjugated polymers: Design, synthesis, and the synergistic effect of the substituent on their solar cell properties[J]. 2020, 137(43): 49342

[3] Guo H., Huang X. X., Liu Z. J., *et al*. Novel polymer donors based on simple A1-π-

A2 structure for non-halogen solvent-processed organic solar cells[J]. Dyes and Pigments, 2021, 196: 109817

[4] Liu Z. J., Chen X. Y., Huang S. R., *et al*. Novel efficient accptor(1)-acceptor(2) type copolymer donors: Vinyl induced planar geometry and high performance organic solar cells[J]. Chemical Engineering Journal, 2021, 419: 129532

[5] Zhang Y. D., Shao Y. M., Wei Z. Y., *et al*. "Double-Acceptor-Type" Random Conjugated Terpolymer Donors for Additive-Free Non-Fullerene Organic Solar Cells[J]. ACS Applied Materials & Interfaces, 2020, 12(18): 20741-20749

[6] Guo H., Huang B., Zhang L. F., *et al*. Double Acceptor Block-Containing Copolymers with Deep HOMO Levels for Organic Solar Cells: Adjusting Carboxylate Substituent Position for Planarity[J]. ACS Applied Materials & Interfaces, 2019, 11(17): 15853-15860

[7] Yu J. W., Chen P., Koh C. W., *et al*. Phthalimide-Based High Mobility Polymer Semiconductors for Efficient Nonfullerene Solar Cells with Power Conversion Efficiencies over 13%[J]. Advanced Science, 2019, 6(2): 1801743

[8] Guo H., Chen L., Huang B., *et al*. Double acceptor block-based copolymers forefficient organic solar cells: side-chain andπ-bridge engineered high open-circuit voltage andsmall driving force[J]. Polymer Chemistry, 2019, 10: 6227-6235

[9] Chang S. W., Muto T., Kondo T., *et al*. Double acceptor donor-acceptor alternating conjugated polymers containing cyclopentadithiophene, benzothiadiazole and thienopyrroledione: toward subtractive color organic photovoltaics[J]. Polymer Journal, 2017, 49(1): 113-122

[10] Jeon S. J., Lee T. H., Han Y. W., *et al*. Design and synthesis of 2D A1-π-A2 copolymers impact on fullerene network for efficient polymer solar cells[J]. Polymer, 2018, 149: 85-95

[11] An Y. K., Liao X. F., Chen L., *et al*. A1-A2 Type Wide Bandgap Polymers for High‐Performance Polymer Solar Cells: Energy Loss and Morphology[J]. Solar RRL, 2019, 3(1): 1800291

[12] Wang X. F., Lv L., Li L. L., *et al*. High-Performance All-Polymer Photoresponse

Devices Based on Acceptor-Acceptor Conjugated Polymers[J]. Advanced Functional Materials, 2016, 26(34): 6306-6315

[13] Ge C. W., Mei C. Y., Ling J., *et al*. Acceptor-Acceptor Conjugated Copolymers Based on Perylenediimide and Benzothiadiazole for All-Polymer Solar Cells[J]. Journal of Polymer Science Part A-Polymer Chemistry, 2014, 52(8): 1200-1215

[14] Shen S, Tu Q, Tao H, *et al*. Side-chain engineering of wide-bandgap copolymers based on two different electron-deficient units for high-performance polymer solar cells[J]. Polymer Chemistry, 2023, 14(36): 4227-4234

[15] Deng J, Huang S, Liu J, *et al*. Layer-by-layer and non-halogenated solvent processing of benzodithiophene-free simple polymer donors for organic solar cells[J]. Chemical Engineering Journal, 2022, 443: 136515

[16] Keshtov M L, Kuklin S A, Khokhlov A R, *et al*. Regular conjugated D-A copolymer containing two benzotriazole and benzothiadiazole acceptors and dithienosilole donor units for photovoltaic application[J]. RSC Adv., 2017, 7(78): 49204-49214

[17] Chen S, Yao H, Li Z, *et al*. Surprising Effects upon Inserting Benzene Units into a Quaterthiophene-Based D-A Polymer-Improving Non-Fullerene Organic Solar Cells via Donor Polymer Design[J]. Advanced Energy Materials, 2017, 7(12): 1602304

[18] Qi F, Song J, Xiong W, *et al*. Two wide-bandgap fluorine-substituted benzotriazole based terpolymers for efficient polymer solar cells[J]. Dyes and Pigments, 2018, 155: 126-134